Journal of Energy Storage 86 (2024) 111318

Contents lists available at ScienceDirect

Journal of Energy Storage

journal homepage: www.elsevier.com/locate/est

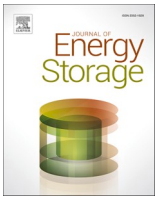

Research papers

A multi-agent-based microgrid day-ahead optimal operation framework with liquid air energy storage by hybrid IGDT-STA

Ruiqiu Yao [a], Hao Xie [b], Chunsheng Wang [b], Xiandong Xu [c], Dajun Du [d], Liz Varga [a], Yukun Hu [a,*]

[a] Department of Civil, Environmental & Geomatic Engineering, University College London, London WC1E 6BT, United Kingdom
[b] School of Automation, Central South University, Changsha 410083, China
[c] School of Electrical and Information Engineering, Tianjin University, Tianjin 300072, China
[d] School of Mechatronics Engineering and Automation, Shanghai University, Shanghai 200072, China

ARTICLE INFO

Keywords:
Optimal operation method
Liquid air energy storage
Information gap decision theory
State transition algorithm
Multi-agent system

ABSTRACT

Liquid air energy storage (LAES) is a promising energy storage technology for net-zero transition. Regarding microgrids that utilize LAES, the price of electricity in the market can create significant uncertainty within the system. To address this issue, the information gap decision theory (IGDT) method has proven to be an effective tool for resolving uncertainties in system operation. The IGDT method is a decision-making tool designed to tackle uncertainty, which can significantly enhance decision-making abilities in situations where information is scarce. Additionally, the state transition algorithm (STA) is a highly intelligent optimization algorithm that leverages structural learning. This study proposed a novel IGDT-STA hybrid method to solve the optimal operation of a microgrid with LAES while considering the uncertainty of market electricity prices. The IGDT-STA offers two distinct strategies for decision-makers who are either risk-averse or risk-taking. These strategies are subsequently optimized by the STA method. In addition, the IGDT-STA is implemented within a multi-agent framework to enhance system flexibility. Through a case study, it was found that the IGDT-STA employed good performance compared with the IGDT-genetic algorithm, stochastic method, and Monte Carlo method.

1. Introduction

Renewable energy sources (RES) have undergone continual advancements due to the economic advantages of cost reduction and the environmental benefits of minimal pollutant emissions [1]. Integrating large-scale energy storage technology is crucial to further enhance the potential of renewable energy [2]. This technology involves storing the physical, chemical, and electromagnetic energy [3]. From the perspective of environmental protection, adopting physical energy storage systems that cause minimal pollution is a promising approach [4]. Among the various physical energy storage technologies available, pumped energy storage, flywheel energy storage, and compressed air energy storage (CAES) are the most popular.

Pumped energy storage transforms electrical energy into mechanical energy, which is then transferred to the potential energy of water. Pumped energy storage has a low investment cost but requires a long construction time and has negative environmental impacts. Additionally, some developed countries cannot use pumped energy storage due to geographical limitations and the limited capacity of large reservoirs [5]. Flywheel energy storage converts electrical energy into rotational kinetic energy of a spinning flywheel that can be regained later. This technology has a long lifespan and high efficiency, but it also has drawbacks such as high capital cost and high self-discharge rate. CAES converts electrical energy into potential energy of compressed air molecules, which are stored in underground caverns or other suitable locations. CASE has a high safety level, but the number of caves or abandoned mines limits its application [6,7]. On the other hand, liquid air energy storage (LAES) is a new large-scale physical energy storage technology that compresses and condenses air into a liquid state in the cryogenic storage tank, as shown in Fig. 1. It should be noted that the round-trip efficiency of LAES ranges from 50 % to 60 %, depending on the system design [8]. Although LAES tends to have lower round trip efficiency than other storage methods, it has the advantages of high energy storage density, accessible storage, and less restricted by geographical conditions compared with CAES.

The research on LAES mainly focuses on thermodynamic and economic analysis [9–12]. Borri et al. [13] conducted a preliminary analysis of different liquefaction cycles and proposed an optimized configuration scheme for liquefaction devices in microgrid-scale LAES. Briola et al.

* Corresponding author.
E-mail address: yukun.hu@ucl.ac.uk (Y. Hu).

https://doi.org/10.1016/j.est.2024.111318
Received 15 September 2023; Received in revised form 5 January 2024; Accepted 10 March 2024
Available online 21 March 2024

Nomenclature

Abbreviations

LAES	Liquid Air Energy Storage
CAES	Compressed Air Energy Storage
IGDT	Information Gap Decision Theory
STA	State Transition Algorithm
GA	Genetic Algorithm
NOCT	Nominal Operating Cell Temperature
SOC	State of Charge
WT	Wind Turbine

Variables

λ	actual value of the uncertain parameter [−]
$\widehat{\lambda}_t$	predicted value of the uncertainty parameter [−]
α	bound for system uncertainty levels [−]
C_{averse}	target system cost that for risk-averse decision-makers [$]
C_{taking}	target system cost that for risk-taking decision-makers [$]
P_{WT}^{t}	WT output power at time t [kW]
G_T	solar radiation incident on the PV [Wm^{-2}]
T_c	PV cell temperature [$^{\circ}C$]
P_{MT}^{t}	output power of micro-turbine at time t [kW]
P_{WT}^{t}	output power of WT at time t [kW]
P_{PV}^{t}	output power of PV at time t [kW]
P_{LAES}^{t}	charge and discharge power of LAES at time t [kW]
P_{gird}^{t}	tie line transition power at time t [kW]

Parameters

ω	rotation operator [−]
β	translation operator [−]
γ	expansion operator [−]
δ	axesion operator [−]
Ψ_{SE}	search enforcement constant [−]
ω_{in}^{cut}	cut-in wind speed [ms^{-1}]
ω_{out}^{cut}	cut-out wind speed [ms^{-1}]
ω_{rate}	rated speed WT [ms^{-1}]
P_{WT}^{rated}	rated power of WT [kW]
P_{PV}^{rated}	rated power of PV [kW]
f_{pv}	derating factor of PV [−]
$G_{T,STC}$	incident radiation at the standard test conditions [Wm^{-2}]
α_p	temperature coefficient [−]
$T_{c,STC}$	PV cell temperature at the standard test conditions [$^{\circ}C$]
$T_{a,NOCT}$	ambient temperature under the NOCT [$^{\circ}C$]
$G_{T,NOCT}$	solar radiation under the NOCT [Wm^{-2}]
η_c	electrical conversion efficiency of PV [%]
$\eta_{Kapitza}$	Kapitza cycle efficiency [%]
$\eta_{cryo-pump}$	cryogenic pump efficiency [%]
$\eta_{turbines}$	turbine efficiency [%]

Function

Γ	system operation cost function [$]
$\widehat{\alpha}(P, C_{averse})$	robustness function [−]
$\widehat{\beta}(P, C_{taking})$	opportunity function [−]

[14] developed an LAES integration method, which can be applied to integrate LAES power plants with thermal power plants to improve the utilization efficiency of stored energy while also improving the economics of thermal power plants. Yazdani et al. [15] investigated the CAES, LAES, and hydrogen energy storage as the energy storage system for wind power plants. Yazdani et al. concluded that LAES has better ecological performance and environmental sustainability than the other two large-scale energy storage based on energy analysis. Xie et al. [16] conducted an LAES case study to assess the economic feasibility of investment in the UK LAES plant construction and determine the optimal scale of operations and operating strategy. Lin et al. [17] designed an arbitrage algorithm based on different operating strategies. The algorithm determined the price threshold every half an hour to decide about charging, discharging, and standby of LAES. Khaloie and Vallee [18] investigated the day ahead optimal dispatch of LAES with liquified natural gas to increase system efficiency.

Although many efforts have been made in the optimization and operation strategy of the LAES system, there are only a few studies on the optimal scheduling of microgrids with LAES at this stage. In addition, the operation strategy of a microgrid is affected by uncertainties from wind and photovoltaic power generation, system load, and market electricity price. At present, the analysis methods of uncertainty problems are as follows: stochastic programming [19], fuzzy theory, robust optimization [20], Interval optimization [21], scenario optimization [22], and information gap decision theory (IGDT) [23]. Marino et al. [24] considered the uncertainty of power demand. They proposed a scalable two-stage stochastic programming model with chance constraints, which minimized the operating cost of the microgrid while ensuring the effective use of renewable energy. Dong et al. [25] proposed an energy management scheme based on adaptive optimal fuzzy logic for the intermittence and randomness of renewable energy and demand. Zhao et al. [26] studied a new two-stage minimum-max-min robust optimal scheduling model, establishing the uncertain set of renewable energy generation and demand loading through robust optimization modeling. Li et al. [27] established a microgrid model considering uncertainty based on interval optimization with the wind power and photovoltaic output as interval variables. Khaloie et al. [28] proposed a new bidding and offering strategy while considering a risk-based operation strategy. Borujeni et al. [29] took renewable energy output and load as uncertain variables, classified them according to seasons, and selected appropriate scene generation methods according to dynamic behaviors, improving microgrid planning reliability.

Choosing an appropriate level of uncertainty for optimization problems is challenging in real-world applications. High uncertainty can raise the system's operating cost, while low uncertainty can compromise the system's stability [30]. Compared with the above methods, the IGDT method is suitable for evaluating various risk levels without statistical data [31]. This method is ideal for systems with difficult or scarce uncertain parameter information. Decision-makers can use the IGDT method to make decisions and enhance their decision-making ability. Moreover, this method can offer different strategies for different needs because it sets both the opportunity and robustness functions to formulate the strategy of risk-averse and risk-taking.

Some researchers have recently used the IGDT method to model the microgrid system. The IGDT method can help the decision-makers choose the most economical and feasible solutions for the microgrid system under uncertainty. Nasr et al. [32] proposed a robust framework based on the IGDT method to realize the effective operation of island microgrids, considering the uncertainty of photovoltaic power generation and demand. Rezaei et al. [33] proposed a new multi-objective auction strategy based on the IGDT method, which managed the severe uncertainty caused by market electricity prices and load fluctuations. As a result, the operating efficiency of the microgrid and spinning reserve market was improved. Khaloie et al. [34] proposed a day-ahead and intra-day risk-controlled multi-objective optimization framework with IGDT. Mehdizadeh et al. [35] proposed a short-term power generation dispatch method for grid-connected microgrids to obtain the optimal bidding strategy, considering the demand response program based on the IGDT method under uncertain upstream grid prices. Based on the abovementioned literature, it can be concluded that the IGDT

method is a suitable and effective energy-dispatching strategy when the microgrid is faced with various resource uncertainties. This study considers the uncertainties in electricity market price as a significant uncertain factor in formulating the optimal dispatch strategy. Thus, this study uses IGDT to model the uncertainties in electricity market prices to ensure the stable and economic operation of the microgrid system.

Recently, many hybrid methods have been proposed, which have attracted wide attention from researchers [36,37]. Cai et al. [38] combined robust optimization and stochastic optimization to establish a novel hybrid method to simulate the uncertainty of the cavern capacity of CAES and the market electricity prices. Among these methods, one major trend is applying intelligent optimization algorithms to optimize uncertain modeling methods. The state transition algorithm (STA) is a new intelligent optimization algorithm based on structuralist learning, first proposed by Zhou, Yang, and Gui [39]. The core concept of STA is treating a solution to an optimization problem as a state. The generation and update process of the solution is treated as a state transition process. The unified framework of the solution process of the algorithm is based on the state space expression in modern control theory, and four state transformation operators are constructed on this framework. Most traditional intelligent optimization algorithms, such as genetic algorithm (GA) [40], particle swarm optimization (PSO) [41], and simulated annealing algorithm (SAA) [42], are mainly inspired by imitating social phenomena or natural laws. Unlike these traditional intelligent optimization algorithms, the state transition algorithm is an intelligent optimization algorithm based on structural learning, which shows better performance than conventional intelligent optimization algorithms [39].

1.1. Research gaps

The existing research on energy system management with IGDT mainly focuses on using convex optimization techniques to solve IGDT problems, as shown in the comprehensive review of IGDT application in energy problems by Majidi, Mohammadi-Ivatloo, and Soroudi [43]. However, only a limited number of studies use heuristic optimization to solve the IGDT problem for energy system management. Nojavan et al. [44], Kim and Kim [37], as well as Ke et al. [45] proposed energy system management strategies by solving IGDT with modified particle swarm optimization algorithms. To the author's knowledge, no studies are investigating how to optimize the IGDT problems with STA in the energy systems. In addition, there is limited research on investigating the optimal operation of a microgrid with LAES with IGDT. As a result, this study proposed a novel IGDT-STA hybrid method to solve the optimal operation of a microgrid with LAES while considering the uncertainty of market electricity prices.

1.2. Contributions

The main contributions of this article are as follows:

1) The IGDT method is implemented on a microgrid with LAES for the first time to solve the optimal operation problem with uncertainty in market electricity prices.
2) This study proposed a novel operational framework that integrates IGDT-STA hybrid method with a multi-agent system to optimize the robustness function and opportunity function in the IGDT.
3) This study compared the proposed IGDT-STA method with genetic algorithm optimization techniques, stochastic method, and Monte Carlo method in a case study. The results showed the effectiveness of IGDT-STA.

This study is divided into five sections. The second section explains the IGDT-STA method. In the third section, considering the uncertainty of electricity prices, the day-ahead optimization model of microgrids with LAES based on the IGDT method is established. The fourth section explains the IGDT-STA method through a case study and compares it with the IGDT-GA method. Finally, in the fifth section, the main conclusions of this paper are drawn.

2. The IGDT-STA method

This section explains the mathematical details of the IGDT-STA method. Section 2.1 describes the IGDT mathematic models, and Section 2.2 includes the mathematical formulation of STA.

2.1. IGDT mathematic models

The IGDT effectively manages system uncertainties by focusing on the information gap. Rather than relying on probability distributions, it specifically addresses the divergence between anticipated and actual values within an uncertainty parameter. As a result, IGDT is able to model uncertainties with a severe lack of information [43]. In addition, it effectively manages system uncertainties by focusing on the information gap. Rather than relying on probability distributions, it specifically addresses the divergence between anticipated and actual values within an uncertainty parameter. Section 2.1 explains the details of the system model, uncertainty model, and performance requirements in IGDT.

1) System models

The decision variables and uncertainty parameters in the decision space and uncertainty space are P and λ, respectively. The system model can be expressed as the optimization problem (1) to minimize the system cost.

$$\begin{aligned} &Minimize \quad C(P,\lambda) \\ &\quad Subject\ to: \\ &G_i(P,\lambda) \geq 0, \quad i = 1,\ldots,m \\ &H_j(P,\lambda) = 0, \quad j = 1,\ldots,n \end{aligned} \tag{1}$$

where $C(P,\lambda)$ is the system cost function which takes decision variable P and uncertainty parameter λ as function input. $G_i(P,\lambda) \geq 0$ and $H_j(P,\lambda) = 0$ are inequality and equality constraints, respectively.

2) Uncertainty models

The uncertainty model of IGDT aims to describe the information gap between the predicted value of the uncertainty parameter and its true value [46]. The uncertainty model can be expressed as Eq. (2):

$$U(\alpha,\widehat{\lambda}_t) = \left\{\lambda_t : \frac{|\lambda_t - \widehat{\lambda}_t|}{\widehat{\lambda}_t} \leq \alpha\right\}, \alpha \geq 0 \tag{2}$$

Where λ_t denotes the actual value of the uncertain parameter. $\widehat{\lambda}_t$ denotes the predicted value of the uncertainty parameter. α is the bound for system uncertainty levels. In essence, the uncertainty model ensures that the deviation of uncertainty parameter λ_t with respect to $\widehat{\lambda}_t$ will not exceed $\alpha\widehat{\lambda}_t$.

3) Performance requirements

The IGDT performance requirements are the quantitative evaluations of objective function performance with respect to system robustness and opportunity values. The performance requirements consist of robustness function Eq. (3) and opportunity function Eq. (4).

$$\begin{aligned} \widehat{\alpha}(P,C_{averse}) &= \max_{\alpha}\{\alpha : \text{maximum cost which is not higher than a specified cost}\} \\ &= \max_{\alpha}\{\alpha : max(C(P,\lambda)) \leq C_{averse}\} \end{aligned} \tag{3}$$

where C_{averse} is the target system cost that risk-averse decision-makers are willing to pay. The function value $\widehat{\alpha}(P, C_{averse})$ indicates the maximum possible system uncertainty with a given cost target C_{averse}. In other words, Eq. (1) returns the maximum fluctuation bound for uncertainty parameter λ. The greater value of $\widehat{\alpha}(P, C_{averse})$ means the system is more robust and less susceptible to uncertainties. Therefore, the risk-averse decision-makers are able to make robust decisions, ensuring the system is resilient against uncertainties.

$$\begin{aligned}\widehat{\beta}\left(P, C_{taking}\right) &= \min_{\alpha}\{\alpha : \text{minimum cost which is less than a specified cost}\} \\ &= \min_{\alpha}\left\{\alpha : min(C(P,\lambda)) \le C_{taking}\right\}\end{aligned} \tag{4}$$

where C_{taking} is the target system cost that risk-taking decision-makers are willing to pay. The opportunity function Eq. (2) returns the minimum fluctuation range of uncertain variables that risk-taker decision-makers usually allow. This function mainly evaluates the positive aspects of uncertainty and finds the minimum uncertainty level that the system can tolerate by reducing costs.

2.2. STA mathematic formulations

The STA method is a heuristic optimization algorithm that treats an optimized solution as a state and the iterative update steps as state transition processes. STA uses the state space representation in modern control theory as a framework to solve optimization problems [39]. In the framework of the STA method, a candidate solution can be treated as a state. STA updats states by state transition operations. With state space representation, the unified form of STA is:

$$\begin{cases} x_{k+1} = A_k x_k + B_k u_k \\ y_{k+1} = f(x_{k+1}) \end{cases} \tag{5}$$

where $f(\cdot)$ denotes the objective function. x_k is the current state which corresponds to a solution to the optimization problem. x_{k+1} is the next state and y_{k+1} is the fitness value at the next state. A_k and B_k denote the state transition matrices, which can be also regarded as state transformation operators. u_k is the function of x_k and the historical state.

With state space representations, the STA method defines four state transformation operators to solve optimization problems.

1) Rotation transformation:

$$x_{k+1} = x_k + \omega \frac{1}{n\|x_k\|_2} R_r x_k \tag{6}$$

where $\omega \in \mathbb{R} > 0$ denotes a rotation operator. $R_r \in \mathbb{R}^{n\times n}$ denotes a random matrix whose entries are uniformly distributed random variables between $[-1, 1]$. $\|\cdot\|_2$ denotes Euclidean norm (or L2 norm) of a vector. The rotation operator has the functionality to search in a hypersphere with the maximum radius ω, which has been proven in [39].

2) Translation transformation:

$$x_{k+1} = x_k + \beta R_t \frac{x_k - x_{k-1}}{\|x_k - x_{k-1}\|_2} \tag{7}$$

where $\beta \in \mathbb{R} > 0$ denotes a translation operator. $R_t \in \mathbb{R}$ denotes a uniformly distributed random variable on interval [0,1]. The translation transformation aims to line search for a possible better candidate solution, which can be regarded as a heuristic operator.

3) Expansion transformation:

$$x_{k+1} = x_k + \gamma R_e x_k \tag{8}$$

where $\gamma \in \mathbb{R} > 0$ denotes an expansion operator. $R_e \in \mathbb{R}^{n\times n}$ denotes a random diagonal matrix under normal distribution. The expansion transformation is designed for global search with probabilities to search the whole space.

4) Axesion transformation:

$$x_{k+1} = x_k + \delta R_a x_k \tag{9}$$

where $\delta \in \mathbb{R} > 0$ denotes an axesion operator. $R_a \in \mathbb{R}^{n\times n}$ denotes a sparse random diagonal matrix under normal distribution and only one random entry is not zero. The axesion transformation has the functionality to strengthen single dimensional search [47].

The STA also incorporated sampling in the optimization process. A representative sampling technique is used to avoid enumerating all potential candidate states [47]. The STA performs a transformation operation with multiple times parameterized by a positive integer Ψ_{SE}, representing search enforcement constant. After explaining the four

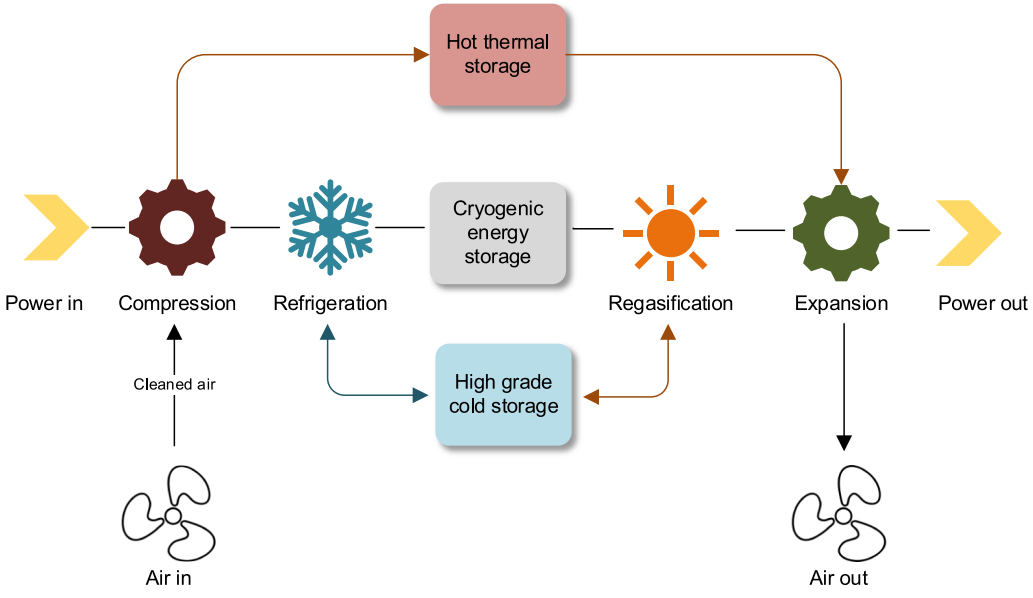

Fig. 1. Schematic diagram of LAES system operation

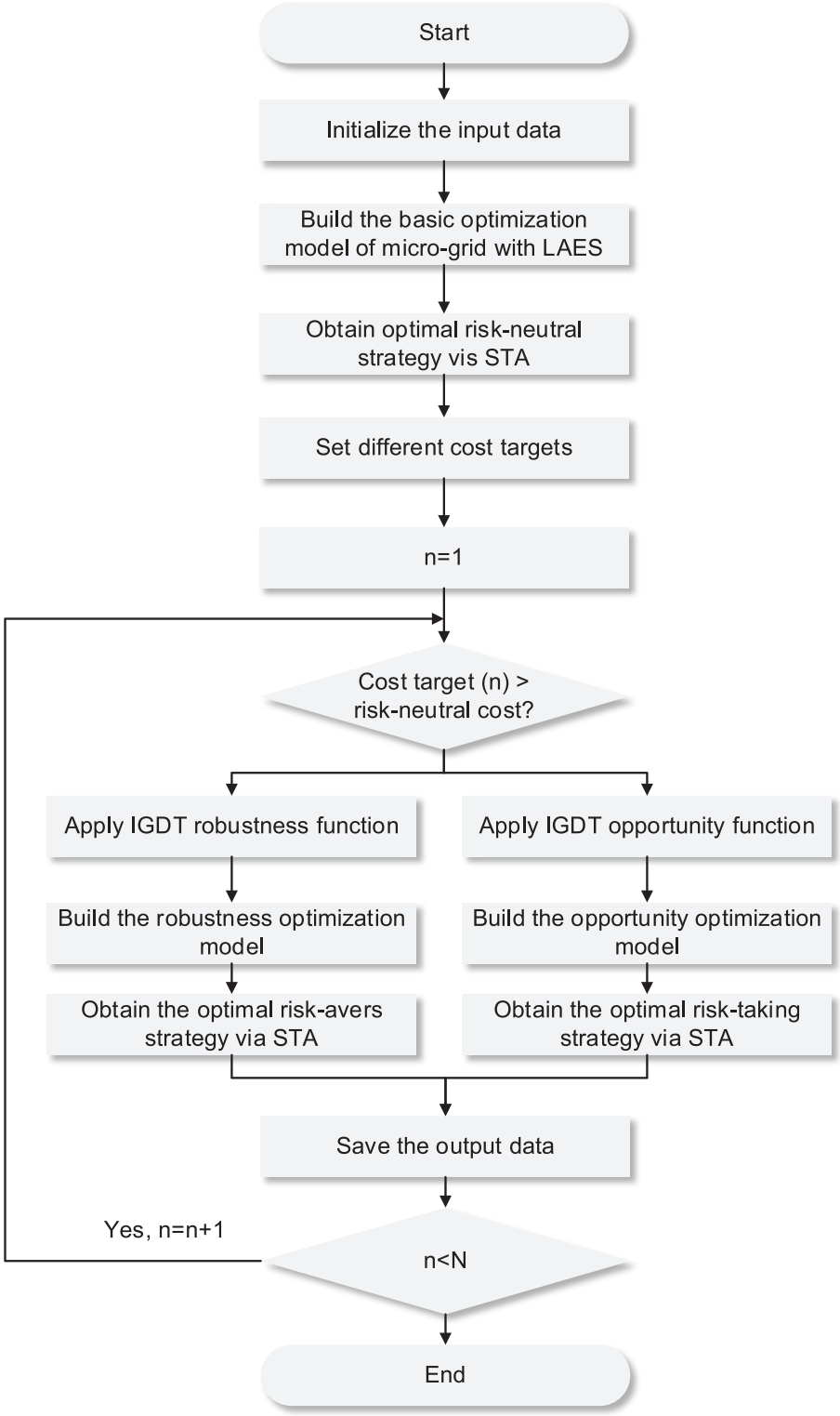

Fig. 2. The flow chart of IGDT-STA.

transformation operations and sampling technique, the STA can be described with the following pseudocodes:

State ← initialization(Ψ_{SE})
Best ← fitness(funfcn, State)
repeat
  if $\omega < \omega_{min}$ **do**
    $\omega \leftarrow \omega_{max}$
  end if
  Best ← expansion(funfcn, Best, Ψ_{SE}, β, γ)
  Best ← rotation (funfcn, Best, Ψ_{SE}, β, ω)
  Best ← axesion (funfcn, Best, Ψ_{SE}, β, δ)
  $\omega \leftarrow \frac{\omega}{fc}$
until the termination criterion is met

The initialization (•) in the above pseudocodes initializes a candidate solution in the feasible set. The fitness (•) selects the best solution with state vector after evaluaton with the objective function. During the optimization process, The rotation operator ω decrease periodically from maximum value ω_{max} to minimum value ω_{min} with a lessening coefficient fc. Noticeably, the translation operation is implemented in othe other three operations once a better candidatesolution is found. Thus, the translation operator β is passed to the other three operations: expansion (•), rotation (•), and axesion (•).

2.3. IGDT-STA hybrid optimization algorithm

The innovative IGDT-STA hybrid method merges the STA into the IGDT's optimization process. This method involves two distinct stages. During the first stage, STA is utilized to optimize a risk-neutral strategy using prediction data. In the second stage, STA optimizes the performance requirement functions of the IGDT, which encompasses both the robustness function and the opportunity function, based on the risk-neutral strategy acquired in the first stage. Accordingly, the microgrid's optimal operation strategy with LAES is developed, accounting for uncertain market electricity prices. Fig. 2 depicts the IGDT-STA method flowchart, and the solution process is summarized as follows:

(1) Input the necessary data of the microgrid system, such as the parameters of wind turbines, photovoltaic arrays, micro gas turbine, LAES, and the predicted value of market electricity price.
(2) The base optimization model of the microgrid with LAES is formulated. This model aims to minimize the operation cost of microgrids with LAES while considering various constraints such as operation constraints of LAES, micro gas turbine, and tie-line transmission power.
(3) The STA method is used to solve the basic optimization model of microgrid with LAES and further obtain the risk-neutral strategy, which is the minimum operating cost strategy of the system based on the predicted market price. The minimum operating cost under this strategy is also called risk-neutral cost.
(4) Different cost targets are set according to the minimum operating cost corresponding to the obtained risk-neutral strategy. The cost targets can be divided into two categories: the cost target greater than the risk-neutral cost and the cost target less than the risk-neutral cost.
(5) The cost target determines thee optimization model of the second stage. The target cost greater than the risk-neutral cost corresponds to the robustness optimization model. The robustness model aims to maximize the robustness function in the IGDT method, and the cost target that is less than the risk-neutral cost corresponds to the opportunity optimization model. The opportunity model aims to minimize the opportunity function in the IGDT method. The above two models both consider the constraints of the system.
(6) The STA method is applied to solve the microgrid's robust or opportunity optimization models with LAES. Further, it obtains the risk-averse strategy or the risk-taker strategy.

3. MAS-based microgrid coordination models

This section describes the details of the MAS-based microgrid coordination model, where the agents solve for optimal operation strategy cooperatively. Section 3.1 explains the structure of the coordination model, and Section 3.2 describes the details of agent tasks.

3.1. Microgrid environment

The microgrid environment, as shown in Fig. 3, includes a power grid agent, load agent, photovoltaic agent, wind turbine agent, micro-turbine agent, LAES agent, and microgrid coordination agent. The power grid agent is responsible for retrieving the day-ahead price information, and the load agent is accountable for forecasting the day-ahead load curves. The details of the remaining agents will be explained in Section 3.2.

3.2. Agent task description

The section explains the task details of the wind turbine agent, the photovoltaic agent, the LAES agent, the micro-turbine agent, and the microgrid coordination agent.

3.2.1. Wind turbine (WT) agents

The WT agent is responsible for supervising the active operation status of the wind turbine generator, sending cost coefficient signals and WT output power P_{WT}^{t} to the microgrid coordination agent at each time period. The WT output power is formulated according to [48]:

$$P_{WT}^{t}(\omega_t) = \begin{cases} 0, & if\ \omega_t \le \omega_{in}^{cut}\ or\ \omega_t \ge \omega_{out}^{cut} \\ \dfrac{\omega_t - \omega_{in}^{cut}}{\omega_{rated} - \omega_{in}^{cut}} P_{WT}^{rated}, & if\ \omega_{in}^{cut} \le \omega_t \le \omega_{rated} \\ P_{WT}^{rated}, & if\ \omega_{rated} \le \omega_t \le \omega_{out}^{cut} \end{cases} \tag{11}$$

where ω_{in}^{cut} and ω_{out}^{cut} are the cut-in and cut-out wind speed respectively. ω_{rated} and P_{WT}^{rated} are the rated speed and power of WT units, respectively. ω_t is the wind speed at time t, whose probability distribution can be modeled with the Weibull probability density function [49]:

$$PDF(\omega_t) = \frac{k}{c}\left(\frac{\omega_t}{c}\right)^{k-1} e^{-\left(\frac{\omega_t}{c}\right)^{k}} \tag{12}$$

where $k \in (0, \infty)$ and $c \in (0, \infty)$ are the shape and scale parameters respectively for Weibull distribution.

3.2.2. Photovoltaic (PV) agents

The PV agent directly supervises the active operation status of PV arrays and reports the operation cost coefficient and PV array output power P_{PV}^{t} to the microgrid coordinated agent. PV array output power is formulated with Eq. (13) [50]:

$$P_{PV}^{out} = P_{PV}^{rated} f_{pv}\left(\frac{G_T}{G_{T,STC}}\right)\left[1+\alpha_p\left(T_c - T_{c,STC}\right)\right] \tag{13}$$

where P_{PV}^{rated} and f_{pv} are the rated power and derating factor of the PV array units respectively. G_T is the solar radiation incident on the PV array units, and $G_{T,STC}$ is the incident radiation at the standard test conditions. α_p is the temperature coefficient of PV power. $T_{c,STC}$ is the PV cell temperature at the standard test conditions. T_c is the PV cell temperature, which can be calculated with Eq. (14) [50,51]:

$$T_c = T_a(t) + G_T\left(\frac{T_{c,NOCT} - T_{a,NOCT}}{G_{T,NOCT}}\right)\left(1 - \frac{\eta_c}{\tau\alpha_{absorb}}\right) \tag{14}$$

where $T_a(t)$ is the ambient temperature. $T_{c,NOCT}$ is the nominal operating cell temperature (NOCT). $T_{a,NOCT}$ and $G_{T,NOCT}$ are the ambient temperature and solar radiation under the NOCT, respectively. η_c is the electrical conversion efficiency of PV array units. τ is the solar transmittance of the cover of PV array units. α_{absorb} is the solar absorptance of the PV array. The final PV output at time t is calculated with an efficient coefficient η_{inv} to P_{PV}^{out} :

$$P_{PV}^{t} = \eta_{inv} P_{PV}^{out} \tag{15}$$

The solar radiation incident is modeled with the Beta distribution [52]:

$$PDF(G_T) = \frac{\Gamma(\alpha+\beta)}{\Gamma(\alpha)+\Gamma(\beta)}(G_T)^{\alpha-1}(1-G_T)^{\beta-1} \tag{16}$$

where $\Gamma(\bullet)$ is the Gamma function [53], $\alpha, \beta \in [0, \infty]$ are shape parameters for Beta distribution.

3.2.3. LAES agents

The LAES agent is responsible for supervising the active operation status of the LAES plant and reporting the operation information to the microgrid coordination agent. The operation information includes the charging phase, storage phase, and discharging phase information. During the charging phase, Kapitza cycle acts as a recuperative process to liquidfy air and charge the cryogenic energy storage with compressors and cryo-turbines [54], where the efficiency of the process is specified in Eq. (17). During the storage phase, the level of cryogenic energy storage is measured by state-of-charge (SOC) balance Eq. (18), considering the energy loss in storage phase with Eq. (19). During the discharge phase, the liquid air for the tank is pumped out by a cryogenic pump and regasified to ambient temperature. The high-pressure air is further heated up by the thermal storage to drive power turbines [55]. The final discharge power is calculated by Eq. (20) and Eq. (21) with consideration of the efficiencies of cryogenic pumps and power turbines.

$$P_{ch-final}(t) = \eta_{Kapitza} \cdot P_{ch}(t) \tag{17}$$

$$SOC_{LAES}(t) = SOC_{LAES}(t-1) + P_{ch-final}(t) - P_{dis-final}(t) - SOC_{LAES}^{loss}(t) \tag{18}$$

$$SOC_{LAES}^{loss}(t) = \gamma_{loss} \cdot SOC_{LAES}(t) \tag{19}$$

$$P_{\text{pump}}(t) = \eta_{cryo-pump} \cdot P_{dis}(t) \tag{20}$$

$$P_{dis-final}(t) = \eta_{turbine} \cdot P_{pump}(t) \tag{21}$$

In addition to the charge, storage, and discharge information listed above, the LAES agent also sends the operational constraints to the microgrid coordination agent. Constraint (C.1) and (C.2) specify the range of charging and discharging ranges of LAES unit, where $x(t)$, $y(t) \in \{0,1\}$. Constraint (C.3) prevents the LAES plant charges and discharges at the same time at the cryogenic tank. Constraint (C.4) indicates the minimum and maximum range of SOC at each time step t.

$$0 \le P_{ch}(t) \le P_{ch}^{max} \cdot x(t) \tag{C.1}$$

$$0 \le P_{dis}(t) \le P_{dis}^{max} \cdot y(t) \tag{C.2}$$

$$x(t) + y(t) \le 1 \tag{C.3}$$

$$SOC_{LAES}^{min} \le SOC_{LAES}(t) \le SOC_{LAES}^{max} \tag{C.4}$$

3.2.4. Micro-turbine (MT) agents

The MT agent is responsible for sending the cost coefficient of the MT generation unit and micro-turbine specifications, including Constraints (C.5) and (C.6), to the microgrid coordination agent. Constraint (C.5) and Constraint (C.6) indicate operational limits and ramping limits of micro-turbine units, respectively.

$$P_{MT}^{min} \le P_{MT}^{t} \le P_{MT}^{max} \tag{C.5}$$

$$\Delta P_{MT}^{min} \le P_{MT}^{t} - P_{MT}^{t-1} \le \Delta P_{MT}^{max} \tag{C.6}$$

where P_{MT}^{min} and P_{MT}^{max} are the minimum and maximum generation output limits. ΔP_{MT}^{min} and ΔP_{MT}^{max} are the minimum and maximum ramping limits.

3.2.5. Microgrid coordination agents

The microgrid coordination agent is responsible for optimizing objective function Eq. (22) with operational information from other agents.

$$\Gamma = \sum_{t=1}^{24}\left(\xi_{MT} \cdot P_{MT}^{t} + \xi_{WT} \cdot P_{WT}^{t} + \xi_{PV} \cdot P_{PV}^{t} + \xi_{LAES} \cdot \left|P_{LAES}^{t}\right| + \lambda_t \cdot P_{gird}^{t}\right) \tag{22}$$

Where Γ denotes the system operation cost; ξ_{MT} denotes the operating cost coefficient of micro-turbines; P_{MT}^{t} denotes the output power of micro-turbine at time t; ξ_{WT} denotes the operating cost coefficient of wind power generation; P_{WT}^{t} denotes the output power of wind power generation at time t; ξ_{PV} denotes the operating cost coefficient of photovoltaic power generation; P_{PV}^{t} denotes the output power of photovoltaic power generation at time t; ξ_{LAES} denotes the operating cost coefficient of LAES; P_{LAES}^{t} denotes the charge and discharge power of LAES at time t, when $P_{LAES}^{t} \ge 0$, it is considered that the LAES is in a discharging state, when $P_{LAES}^{t} < 0$, the LAES is in a charging state; λ_t denotes the market price of electricity at time t; P_{gird}^{t} denotes the tie line transition power at time t, when $P_{gird}^{t} \ge 0$ the microgrid purchases power from the upper grid.

Once the objective function Eq. (22) is established, the microgrid coordination agent considers decision-makers' risk preferences, including risk-averse and risk-taking options. Risk-averse decision-makers are concerned with the system robustness that can be quantified with the robustness function of IGDT. The robustness function value $\widehat{\alpha}(P, C_{averse})$ represents the maximum uncertainty level corresponding to the risk-averse cost target C_{averse}. On the other hand, risk-taking decision-makers aim to spend as little cost as possible to keep the system running smoothly. The decision is based on the opportunity function, where the opportunity function value $\widehat{\beta}(P, C_{taking})$ represents the minimum level of uncertainty under the risk-taking cost target C_{taking}.

- Problem formulation with risk-averse decision-makers

For risk-averse decision-makers, the micro-grid coordination agent considers the uncertainty of electricity prices to establish a robustness function for the microgrid system. According to the uncertainty model Eq. (2), the high market electricity price can be expressed as:

$$\lambda_t = (1+\alpha)\widehat{\lambda}_t \tag{23}$$

Substituting Eq. (23) into the operating cost function Eq. (22):

$$\Gamma_{averse} = \sum_{t=1}^{24}\left(\xi_{MT}\left(P^t_{MT}\right) + \xi_{WT}\left(P^t_{WT}\right) + \xi_{PV}\left(P^t_{PV}\right) + \xi_{LAES}\left(P^t_{LAES}\right) + (1+\alpha)\widehat{\lambda}_t \cdot P^t_{gird}\right) \tag{24}$$

Substitute the given maximum cost target C_{averse} into Eq. (24):

$$\alpha(P, C_{averse}) = \frac{\sum_{t=1}^{24}\left(\xi_{MT}\left(P^t_{MT}\right) + \xi_{WT}\left(P^t_{WT}\right) + \xi_{PV}\left(P^t_{PV}\right) + \xi_{LAES}\left(P^t_{LAES}\right) + \widehat{\lambda}_t P^t_{gird}\right) - C_{averse}}{-\sum_{t=1}^{24}\widehat{\lambda}_t P^t_{gird}} \tag{25}$$

C_{averse} is the target system cost that risk-averse decision-makers are willing to pay. As explained in Section 2.1, the principle of risk-averse strategy is to obtain the maximum robustness function value $\widehat{\alpha}(P, C_{averse})$ under the cost target C_{averse}. The microgrid coordination agent optimizes the following optimization problem (26):

$$Maximize\left\{\frac{\sum_{t=1}^{24}\left(\xi_{MT}\left(P^t_{MT}\right) + \xi_{WT}\left(P^t_{WT}\right) + \xi_{PV}\left(P^t_{PV}\right) + \xi_{LAES}\left(P^t_{LAES}\right) + \widehat{\lambda}_t P^t_{gird}\right) - C_{averse}}{-\sum_{t=1}^{24}\widehat{\lambda}_t P^t_{gird}}\right\} \tag{26}$$

subject to Constraints (C.1) to (C.6), as well as:

$$P^t_{MT} + P^t_{WT} + P^t_{PV} + P^t_{LAES} + P^t_{grid} = P^t_{load} \tag{C.7}$$

$$P^{min}_{grid} \le P^t_{grid} \le P^{max}_{grid} \tag{C.8}$$

- Problem formulation with risk-taking decision-makers

For risk-taking decision-makers, the micro-gird coordination agent aims to minimize the opportunity function value $\widehat{\beta}(P, C_{taking})$, which solves the minimum fluctuation range of electricity market price. According to uncertain model of IDGT, the expression of low market electricity price can be expressed as:

$$\lambda_t = (1-\alpha)\widehat{\lambda}_t \tag{27}$$

Substituting Eq. (27) into operating cost function Eq. (22):

$$\Gamma_{taking} = \sum_{t=1}^{24}\left(\xi_{MT}\left(P^t_{MT}\right) + \xi_{WT}\left(P^t_{WT}\right) + \xi_{PV}\left(P^t_{PV}\right) + \xi_{LAES}\left(P^t_{LAES}\right) + (1-\alpha)\widehat{\lambda}_t \cdot P^t_{gird}\right) \tag{28}$$

Substitute the given minimum cost target C_{taking} into the Eq. (28):

$$\alpha(P, C_{taking}) = \frac{\sum_{t=1}^{24}\left(\xi_{MT}\left(P^t_{MT}\right) + \xi_{WT}\left(P^t_{WT}\right) + \xi_{PV}\left(P^t_{PV}\right) + \xi_{LAES}\left(P^t_{LAES}\right) + \widehat{\lambda}_t P^t_{gird}\right) - C_{taking}}{\sum_{t=1}^{24}\widehat{\lambda}_t P^t_{gird}} \tag{29}$$

Then, the micro-grid coordination agent solves the optimization problem (30):

$$Minimize\left\{\frac{\sum_{t=1}^{24}\left(\xi_{MT}\left(P^t_{MT}\right) + \xi_{WT}\left(P^t_{WT}\right) + \xi_{PV}\left(P^t_{PV}\right) + \xi_{LAES}\left(P^t_{LAES}\right) + \widehat{\lambda}_t P^t_{gird}\right) - C_{taking}}{\sum_{t=1}^{24}\widehat{\lambda}_t P^t_{gird}}\right\} \tag{30}$$

subject to Constraints (C.1) to (C.8).

Subsequently, the micro-grid coordination agent uses STA to optimize the optimization problem (26) or (30), based on the risk preference of decision-makers.

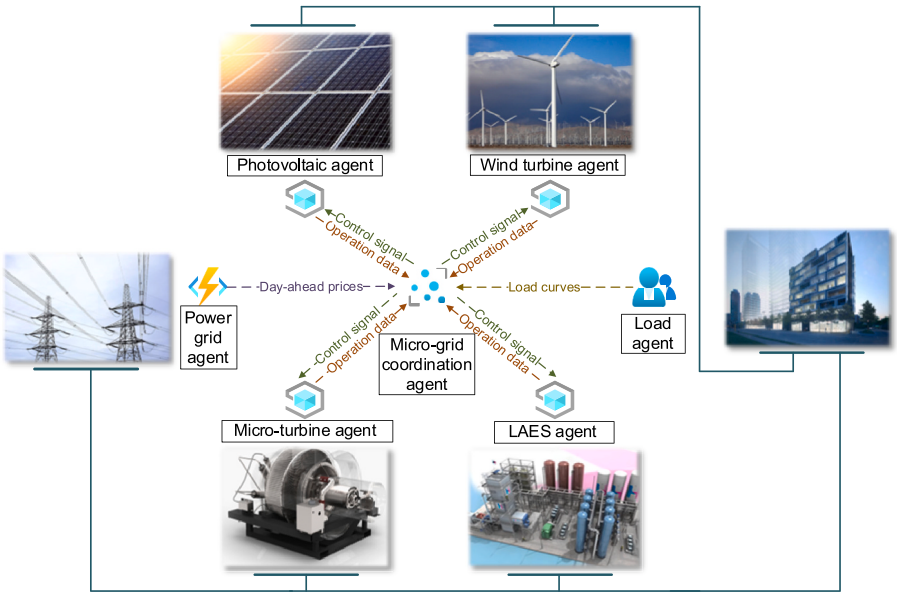

Fig. 3. Schematic diagram of the microgrid with multi-agent system.

4. Case studies

In this study, the optimization of microgrid operation strategy with LAES is formulated under different target costs while considering the uncertainty of market electricity prices. The microgrid system analyzed in this study is a grid-connected one. It comprises a photovoltaic system, a wind power system, a micro gas turbine system and an LAES system. In the case of the LAES system, it is assumed that the pressure ratio of the compressor and expander in each stage remains constant.

4.1. Data preparation

The predicted market price of electricity is shown in Fig. 4. This study assumes that the electricity price sold to the grid is equal to the electricity price purchased from the grid. The system parameters are presented in Table 1. The efficiencies of the LAES plant are obtained from LAES performance research [13,54]. The load power data comes from a microgrid in Northwest China, as shown in Fig. 5. The forecast data for wind power and photovoltaic power are shown in Fig. 6.

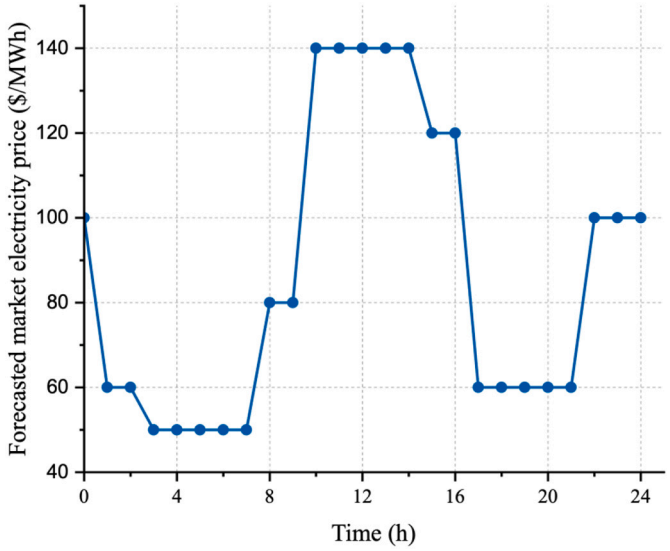

Fig. 4. Forecasted market electricity price.

Table 1
System specifications.

Parameter	Value	Parameter	Value
WT system		*LAES system*	
P_{WT}^{rated}	3000 kW	P_{LAES}^{max}	5 MW
ω_{in}^{cut}	3 ms^{-1}	P_{LAES}^{min}	−5 MW
ω_{out}^{cut}	25ms^{-1}	SOC_{LAES}^{max}	20 MW
ω_{rated}	13 ms^{-1}	SOC_{LAES}^{min}	0.5 MW
ξ_{WT}	0.029 $/kWh	$\eta_{Kapitza}$	85 %
PV system		$\eta_{cryo-pump}$	80 %
P_{PV}^{rated}	3000 kW	$\eta_{turbines}$	80 %
f_{pv}	80 %	γ_{loss}	2 %
α_p	−0.5	ξ_{LAES}	0.025$/kWh
$T_{c,NOCT}$	47 $^{\circ}C$	*MT system*	
$T_{c,STC}$	25 $^{\circ}C$	P_{MT}^{max}	3000 kW
η_c	13 %	P_{MT}^{min}	500 kW
τ	0.0148 MW m^{-2} K^{-1}	ξ_{MT}	0.044 $/kWh
α_{absorb}	30 %	*Other parameters*	
η_{inv}	90 %	P_{grid}^{max}	3000 kW
ξ_{PV}	0.026 $/kWh	P_{grid}^{min}	−3000 kW

4.2. Risk-neutral results

As illustrated in the Section 2.3, the first stage of the IGDT-STA method is to obtain a risk-neutral strategy. In other words, the robustness and opportunity function values are 0 ($\widehat{\alpha} = \widehat{\beta} = 0$). This risk-neutral strategy is obtained by assuming the realized electricity prices are equal to the predicted electricity prices. To demonstrate the effectiveness of the proposed IGDT-STA method, this study uses the Genetic Algorithm (GA) as a reference optimization technique. In addition, this study also compares the risk-neutral strategy with the stochastic method and Monte Carlo method, as demonstrated in [56–58].

Table 2 shows the expected system operation cost of IGDT-STA, IGST-GA, stochastic method, and Monte Carlo method. IGDT-STA method yields a lower operation cost than the remaining methods. Comparing with IGDT-GA, IGDT-STA can reduce the system operation cost for $1538.6. This result demonstrated that STA have better performance than GA for IGDT optimization. It should be noted that the risk neutral strategy means that $\widehat{\alpha}(\$7848.0) = \widehat{\beta}(\$7848.0) = 0$ for IGDT-STA and $\widehat{\alpha}(\$9386.6) = \widehat{\beta}(\$9386.6) = 0$ for IGST-GA. Furthermore, IGDT-STA also yields lower system operation costs than the stochastic method and Monte Carlo method with $900.7 and $892.3 reductions, respectively.

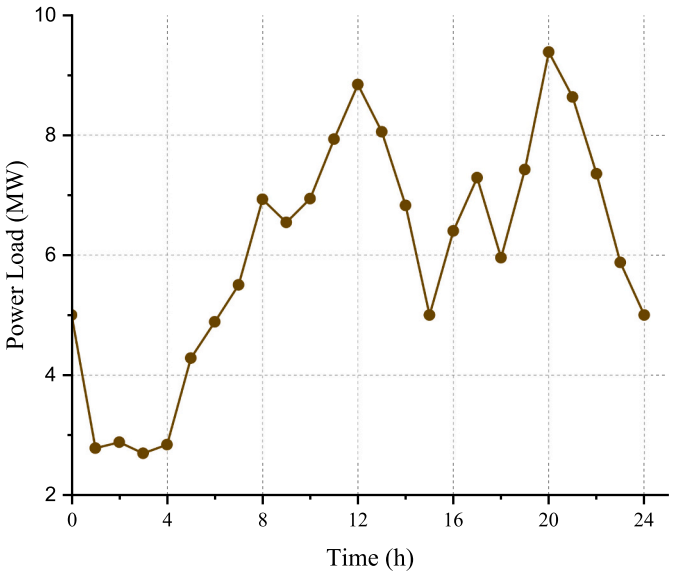

Fig. 5. Power load demand.

As a result, IGDT-STA shows satisfactory results for decision-making under uncertainties.

The hourly expected operating costs based on the four methods are shown in Fig. 7. It can be seen from the figures that the expected operating costs of the IGDT-STA method are mainly reduced during the 13th and 15th hour of the day compared with the remaining three methods. The microgrid operation strategies corresponding to the four methods are shown in Fig. 8(a) to Fig. 8(d), respectively. With respect to the utilization of the LAES plant, all four operation strategies actively use the storage facility to throughout the day. It can be seen from Fig. 8 (a) that IGDT-STA operation strategy changes LAES in the morning and discharges the stored power during the peak load in the noon and evening time. In addition, compared with the IGDT-GA method, the operation strategy based on the IGDT-STA method has more output of the micro gas turbine, thereby reducing the purchase of electricity from the main grid.

4.3. Risk-based results

The robustness $\widehat{\alpha}(\bullet)$ and opportunity $\widehat{\beta}(\bullet)$ function explained in Section 2.1 were employed to form the risk-averse strategy and risk-taking strategy. The results of the risk-averse strategy and risk-taking strategy with different target costs are shown in Fig. 9. A risk-taking decision-maker aims to maximize the opportunity function with a smaller target cost than the risk-neutral cost. The trend of $\widehat{\beta}(C_{taking})$ with respect to C_{taking} is plotted in Fig. 9(a). In this study, the cost step is set to 3 % of the risk-neutral operating cost, i.e. \$281.60 for the IGDT–GA method and \$235.44 for the IGDT–STA method. It is evident that $\widehat{\beta}(C_{taking})$ increases with risk-taking targe cost C_{taking} decreseas for both IGDT-STA and IGDT-GA. Upon comparing the results of IGDT-STA and IGDT-GA, the IGDT-STA method yields a lower $\widehat{\beta}(C_{taking})$ than IGDT-STA. For instance, at an opportunity cost of \$7612.0, the IGDT-STA method has an opportunity coefficient of 0.1399, while the IGDT-GA method has an opportunity coefficient of 0.3744. These results show that IGDT-STA could obtain a risk-taking strategy with less uncertainty compared to the IGDT-GA method.

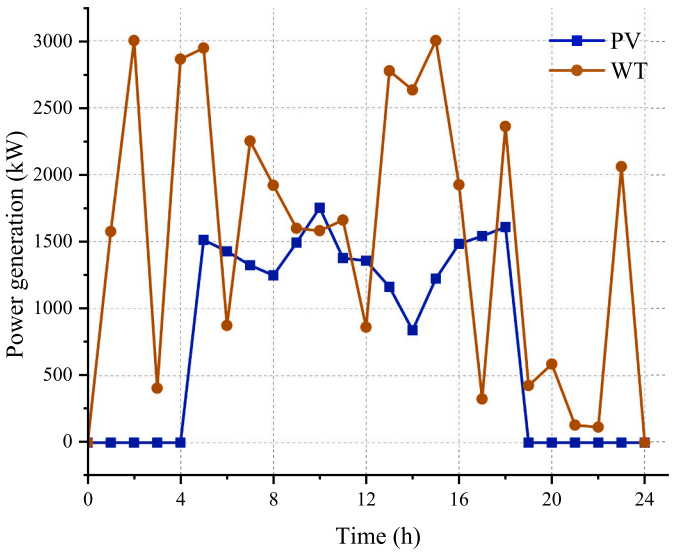

Fig. 6. The output power of PV and WT.

Fig. 9(b) shows the relationship curve between the robustness cost and the robustness coefficient $\widehat{\alpha}(C_{averse})$, which can be obtained based on optimization problem (26). In this study, the cost step is set to 3 % of the risk-neutral operating cost. It is evident that the robustness coefficient rises $\widehat{\alpha}(C_{averse})$ as the robustness cost increases, regardless of the methodology employed. This suggests that the robustness of the system is enhanced with increased operation costs. Notably, the proposed IGDT-STA approach displays greater robustness than IGDT-GA. For example, at a robustness cost of \$10,089.0, the IGDT-STA method has a robustness coefficient of 0.3741, while the IGDT-GA method only has a coefficient of 0.0567. Thus, if the decision-maker favors risk aversion, they can make resilient choices by accepting higher operating costs.

5. Conclusions

Because the LAES system is a promising large-scale energy storage technology without geographical limitation, this study researches the optimal operation strategy of a microgrid with LAES. When formulating the optimal operation strategy to reduce the operation cost of the system and considering the impact of the uncertainty of market electricity price, a day-ahead optimal operation method of microgrid with LAES based on IGDT-STA is proposed. The method is mainly divided into two stages. Firstly, the STA method is used to optimize the risk-neutral strategy. Then, based on the obtained operation strategy, the STA method is used to optimize the robustness and opportunity function in the IGDT method. The case study results show that compared with the IGDT-GA method, stochastic method, and Monte Carlo method, the IGDT-STA method obtains a lower system operation cost of \$7848. In the second stage, the IGDT-STA method shows a higher robustness coefficient and lower opportunity coefficient than IGDT-GA, offering stronger robustness and better opportunity. Future research could further investigate the following two directions: 1) The information gap decision theory is only used for the uncertainties in the market electricity price in this study. Future studies could investigate the potential applications of IGDT on the coupled uncertainties from renewable energy generation and market electricity price. 2) This study treats liquid air energy storage as a steady system. Future research could treat the LAES system as a dynamic system to investigate the dynamic performance of compressors and expanders between different dispatch strategies.

Table 2
Expected operation cost comparison.

	IGDT–STA method	IGDT–GA method	Stochastic method	Monte carlo method
Expected operation cost (\$)	7848.0	9386.6	8748.7	8740.3

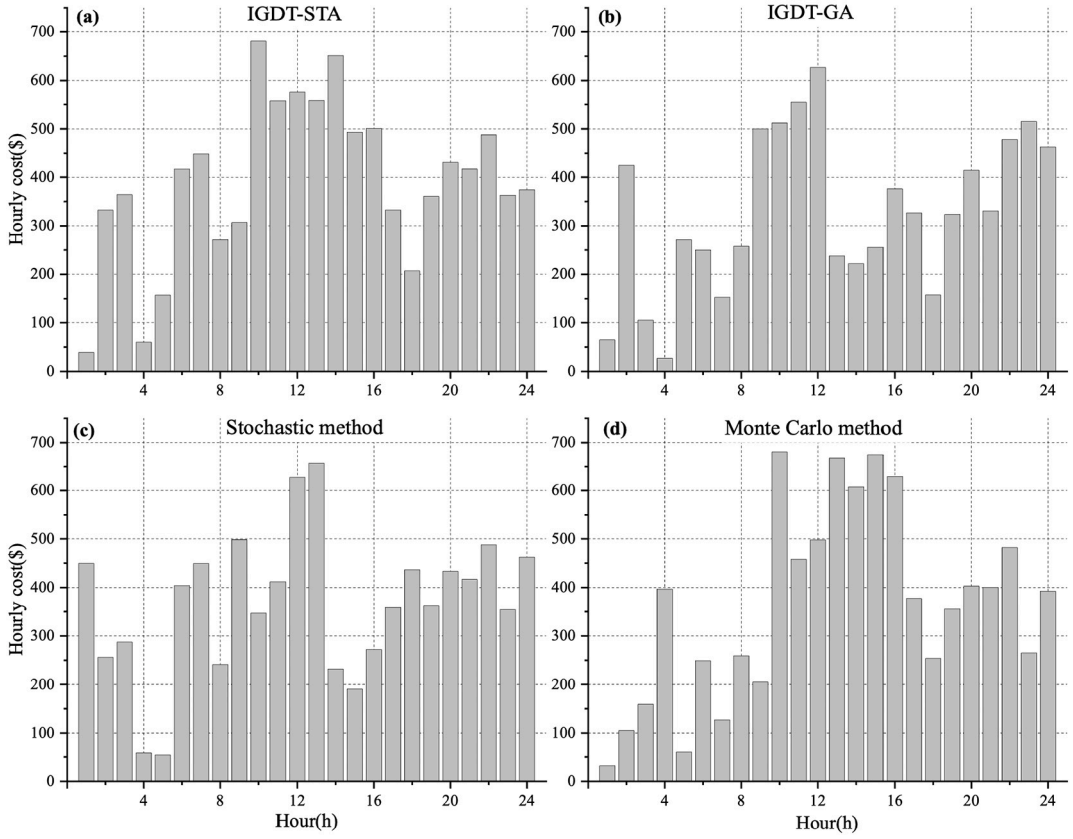

Fig. 7. hourly cost of (a) IGDT-STA method; (b) IGDT-GA method; (c) Stochastic method; (d) Monte Carlo method.

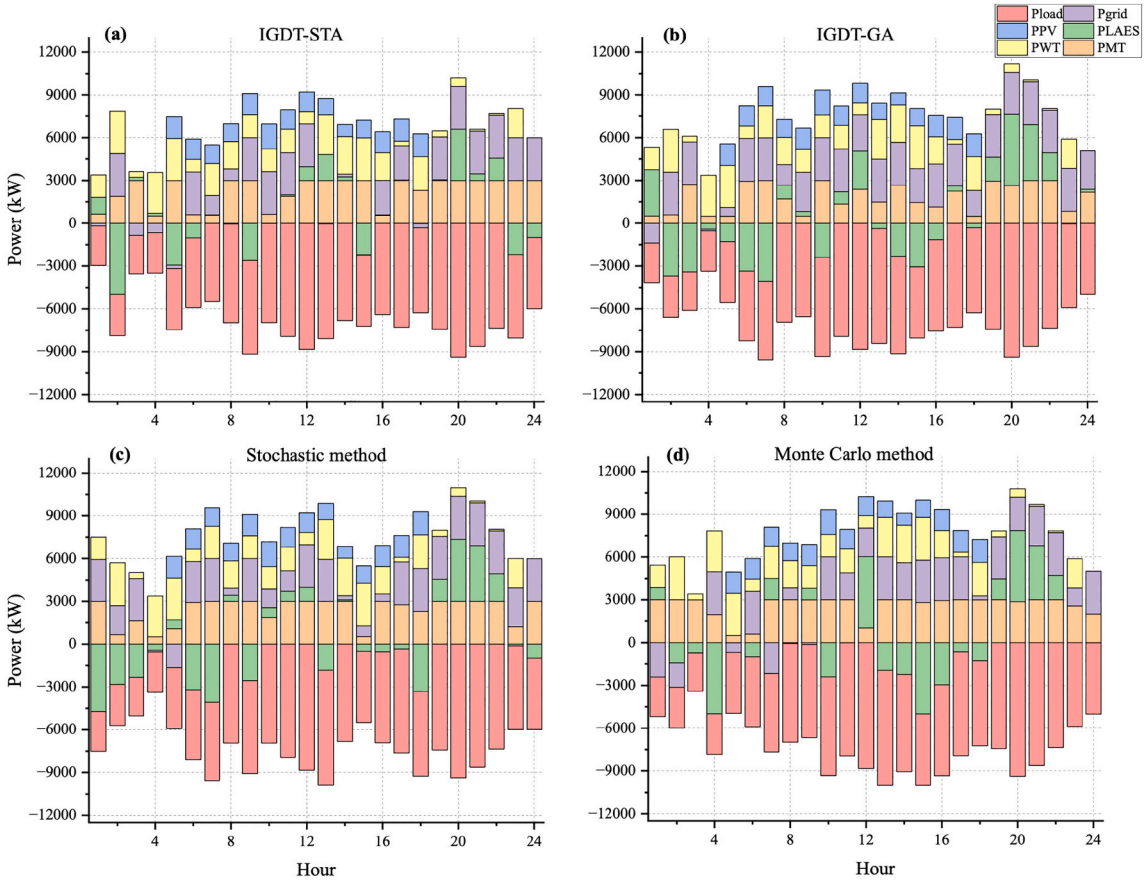

Fig. 8. Microgrid operation strategy based on (a) IGDT-STA; (b) IGDT–GA; (c) Stochatic method; (d) Monte Carlo Method.

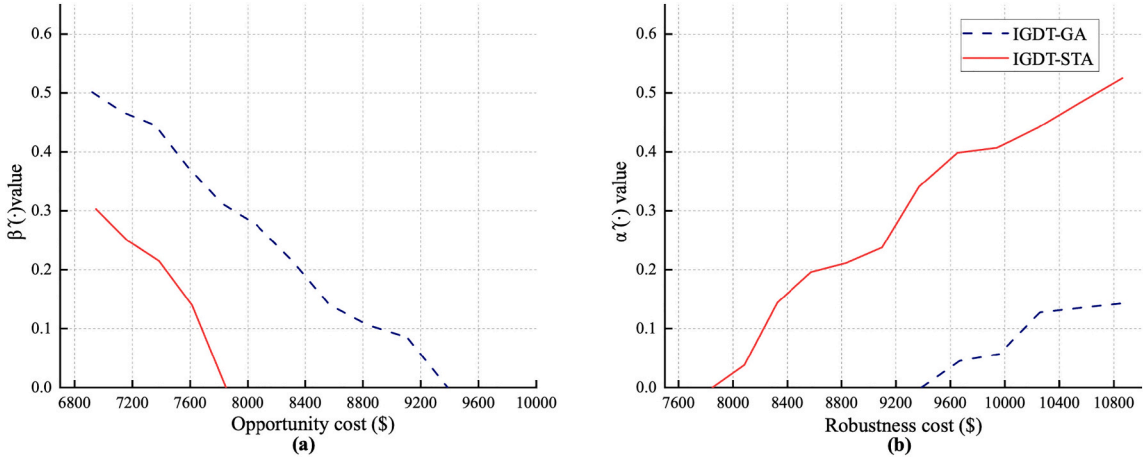

Fig. 9. Opportunity curve and robusteness curve with IGDT-STA and IGDT-GA.

CRediT authorship contribution statement

Ruiqiu Yao: Conceptualization, Methodology, Writing – original draft. **Hao Xie:** Conceptualization, Methodology, Writing – original draft. **Chunsheng Wang:** Supervision, Writing – review & editing. **Xiandong Xu:** Data curation, Investigation. **Dajun Du:** Data curation, Investigation. **Liz Varga:** Project administration, Supervision. **Yukun Hu:** Funding acquisition, Project administration, Supervision, Writing – review & editing.

Declaration of competing interest

The authors declare that they have no competing financial interests or personal relationships that could have appeared to influence the work reported in this paper.

Data availability

Data will be made available on request.

Acknowledgements

This work was supported by National Natural Science Foundation of China (61973322) and The Royal Society of UK (IES\R3\213189).

References

[1] M.A. Jirdehi, V.S. Tabar, S. Ghassemzadeh, S. Tohidi, Different aspects of microgrid management: a comprehensive review, J Energy Storage 30 (2020), https://doi.org/10.1016/j.est.2020.101457.
[2] M. Antonelli, S. Barsali, U. Desideri, R. Giglioli, F. Paganucci, G. Pasini, Liquid air energy storage: potential and challenges of hybrid power plants, Appl. Energy 194 (2017) 522–529, https://doi.org/10.1016/j.apenergy.2016.11.091.
[3] S. Koohi-Fayegh, M.A. Rosen, A review of energy storage types, applications and recent developments, J Energy Storage 27 (2020), https://doi.org/10.1016/j.est.2019.101047.
[4] S. Sabihuddin, A.E. Kiprakis, M. Mueller, A numerical and graphical review of energy storage technologies, Energies (Basel) 8 (2015) 172–216, https://doi.org/10.3390/en8010172.
[5] B. Ameel, C. T'Joen, K. De Kerpel, P. De Jaeger, H. Huisseune, M. Van Belleghem, M. De Paepe, Thermodynamic analysis of energy storage with a liquid air Rankine cycle, Appl. Therm. Eng. 52 (2013) 130–140, https://doi.org/10.1016/j.applthermaleng.2012.11.037.
[6] C. Damak, D. Leducq, H.M. Hoang, D. Negro, A. Delahaye, Liquid Air Energy Storage (LAES) as a large-scale storage technology for renewable energy integration – a review of investigation studies and near perspectives of LAES, Int. J. Refrig. 110 (2020) 208–218, https://doi.org/10.1016/j.ijrefrig.2019.11.009.
[7] J.Y. Heo, J.H. Park, J.I. Lee, Experimental investigation of tank stratification in liquid air energy storage (LAES) system, Appl. Therm. Eng. 202 (2022), https://doi.org/10.1016/j.applthermaleng.2021.117841.
[8] X. She, X. Peng, B. Nie, G. Leng, X. Zhang, L. Weng, L. Tong, L. Zheng, L. Wang, Y. Ding, Enhancement of round trip efficiency of liquid air energy storage through effective utilization of heat of compression, Appl. Energy 206 (2017) 1632–1642, https://doi.org/10.1016/j.apenergy.2017.09.102.
[9] E. Borri, A. Tafone, A. Romagnoli, G. Comodi, A review on liquid air energy storage: history, state of the art and recent developments, Renew. Sust. Energ. Rev. 137 (2021), https://doi.org/10.1016/j.rser.2020.110572.
[10] S. Cui, Q. He, Y. Liu, T. Wang, X. Shi, D. Du, Techno-economic analysis of multi-generation liquid air energy storage system, Appl. Therm. Eng. 198 (2021), https://doi.org/10.1016/j.applthermaleng.2021.117511.
[11] Y. Zhou, L. Duan, X. Ding, Y. Bao, F. Tian, Economic feasibility assessment of a solar aided liquid air energy storage system with different operation strategies, J Energy Storage 72 (2023), https://doi.org/10.1016/j.est.2023.108812.
[12] K. Su, H. Du, X. Zhao, X. Wang, X. Zhang, Y. Lu, X. She, C. Wang, Tech-economic analysis of liquid air energy storage - a promising role for carbon neutrality in China, J Energy Storage 72 (2023), https://doi.org/10.1016/j.est.2023.108786.
[13] E. Borri, A. Tafone, A. Romagnoli, G. Comodi, A preliminary study on the optimal configuration and operating range of a "microgrid scale" air liquefaction plant for Liquid Air Energy Storage, Energy Convers. Manag. 143 (2017) 275–285, https://doi.org/10.1016/j.enconman.2017.03.079.
[14] S. Briola, R. Gabbrielli, A. Delgado, Energy and economic performance assessment of the novel integration of an advanced configuration of liquid air energy storage plant with an existing large-scale natural gas combined cycle, Energy Convers. Manag. 205 (2020), https://doi.org/10.1016/j.enconman.2019.112434.
[15] S. Yazdani, M. Deymi-Dashtebayaz, E. Salimipour, Comprehensive comparison on the ecological performance and environmental sustainability of three energy storage systems employed for a wind farm by using an emergy analysis, Energy Convers. Manag. 191 (2019) 1–11, https://doi.org/10.1016/j.enconman.2019.04.021.
[16] C. Xie, Y. Hong, Y. Ding, Y. Li, J. Radcliffe, An economic feasibility assessment of decoupled energy storage in the UK: with liquid air energy storage as a case study, Appl. Energy 225 (2018) 244–257, https://doi.org/10.1016/j.apenergy.2018.04.074.
[17] B. Lin, W. Wu, M. Bai, C. Xie, Liquid air energy storage: Price arbitrage operations and sizing optimization in the GB real-time electricity market, Energy Econ. 78 (2019) 647–655, https://doi.org/10.1016/j.eneco.2018.11.035.
[18] H. Khaloie, F. Vallee, Day-ahead dispatch of liquid air energy storage coupled with LNG regasification in electricity and LNG markets, IEEE Trans. Power Syst. (2023), https://doi.org/10.1109/TPWRS.2023.3324150.
[19] R. Zhang, G. Li, T. Jiang, H. Chen, X. Li, W. Pei, H. Xiao, Incorporating production task scheduling in energy management of an industrial microgrid: a regret-based stochastic programming approach, IEEE Trans. Power Syst. 36 (2021) 2663–2673, https://doi.org/10.1109/TPWRS.2020.3037831.
[20] Y. Qiu, Q. Li, L. Huang, C. Sun, T. Wang, W. Chen, Adaptive uncertainty sets-based two-stage robust optimisation for economic dispatch of microgrid with demand response, IET Renew. Power Gen. 14 (2020) 3608–3615, https://doi.org/10.1049/iet-rpg.2020.0138.
[21] W. Liu, C. Liu, Y. Lin, K. Bai, L. Ma, Interval multi-objective optimal scheduling for redundant residential microgrid with VESS, IEEE Access 7 (2019) 87849–87865, https://doi.org/10.1109/ACCESS.2019.2923612.
[22] W. Li, R. Wang, T. Zhang, M. Ming, H. Lei, Multi-scenario microgrid optimization using an evolutionary multi-objective algorithm, Swarm Evol. Comput. 50 (2019), https://doi.org/10.1016/j.swevo.2019.100570.
[23] X. Cao, J. Wang, B. Zeng, A chance constrained information-gap decision model for multi-period microgrid planning, IEEE Trans. Power Syst. 33 (2018) 2684–2695, https://doi.org/10.1109/TPWRS.2017.2747625.
[24] C. Marino, M.A. Quddus, M. Marufuzzaman, M. Cowan, A.E. Bednar, A chance-constrained two-stage stochastic programming model for reliable microgrid operations under power demand uncertainty, Sustain. Energy Grids Netw. 13 (2018) 66–77, https://doi.org/10.1016/j.segan.2017.12.007.
[25] W. Dong, Q. Yang, X. Fang, W. Ruan, Adaptive optimal fuzzy logic based energy management in multi-energy microgrid considering operational uncertainties, Appl. Soft Comput. 98 (2021), https://doi.org/10.1016/j.asoc.2020.106882.
[26] B. Zhao, H. Qiu, R. Qin, X. Zhang, W. Gu, C. Wang, Robust optimal dispatch of AC/DC hybrid microgrids considering generation and load uncertainties and energy storage loss, IEEE Trans. Power Syst. 33 (2018) 5945–5957, https://doi.org/10.1109/TPWRS.2018.2835464.
[27] Y. Li, P. Wang, H.B. Gooi, J. Ye, L. Wu, Multi-objective optimal dispatch of microgrid under uncertainties via interval optimization, IEEE Trans. Smart Grid 10 (2019) 2046–2058, https://doi.org/10.1109/TSG.2017.2787790.
[28] H. Khaloie, A. Anvari-Moghaddam, N. Hatziargyriou, J. Contreras, Risk-constrained self-scheduling of a hybrid power plant considering interval-based intraday demand response exchange market prices, J. Clean. Prod. 282 (2021), https://doi.org/10.1016/j.jclepro.2020.125344.
[29] M. Salehi Borujeni, A. Akbari Foroud, A. Dideban, Accurate modeling of uncertainties based on their dynamics analysis in microgrid planning, Sol. Energy 155 (2017) 419–433, https://doi.org/10.1016/j.solener.2017.06.037.
[30] X. Dai, Y. Wang, S. Yang, K. Zhang, IGDT-based economic dispatch considering the uncertainty of wind and demand response, IET Renew. Power Gen. 13 (2019) 856–866, https://doi.org/10.1049/iet-rpg.2018.5581.
[31] M.A. Nasr, E. Nasr-Azadani, H. Nafisi, S.H. Hosseinian, P. Siano, Assessing the effectiveness of weighted information gap decision theory integrated with energy management systems for isolated microgrids, IEEE Trans. Industr. Inform. 16 (2020) 5286–5299, https://doi.org/10.1109/TII.2019.2954706.
[32] M.A. Nasr, E. Nasr-Azadani, A. Rabiee, S.H. Hosseinian, Risk-averse energy management system for isolated microgrids considering generation and demand uncertainties based on information gap decision theory, IET Renew. Power Gen. 13 (2019) 940–951, https://doi.org/10.1049/iet-rpg.2018.5856.
[33] N. Rezaei, A. Ahmadi, A. Khazali, J. Aghaei, Multiobjective risk-constrained optimal bidding strategy of smart microgrids: an IGDT-based normal boundary intersection approach, IEEE Trans. Industr. Inform. 15 (2019) 1532–1543, https://doi.org/10.1109/TII.2018.2850533.
[34] H. Khaloie, F. Vallee, C.S. Lai, J.F. Toubeau, N. Hatziargyriou, Day-ahead and intraday dispatch of an integrated biomass-concentrated solar system: a multi-objective risk-controlling approach, IEEE Trans. Power Syst. 37 (2022) 701–714, https://doi.org/10.1109/TPWRS.2021.3096815.
[35] A. Mehdizadeh, N. Taghizadegan, J. Salehi, Risk-based energy management of renewable-based microgrid using information gap decision theory in the presence of peak load management, Appl. Energy 211 (2018) 617–630, https://doi.org/10.1016/j.apenergy.2017.11.084.
[36] X. Shi, A. Dini, Z. Shao, N.H. Jabarullah, Z. Liu, Impacts of photovoltaic/wind turbine/microgrid turbine and energy storage system for bidding model in power system, J. Clean. Prod. 226 (2019) 845–857, https://doi.org/10.1016/j.jclepro.2019.04.042.
[37] H.J. Kim, M.K. Kim, Risk-based hybrid energy management with developing bidding strategy and advanced demand response of grid-connected microgrid based on stochastic/information gap decision theory, Int. J. Electr. Power Energy Syst. 131 (2021), https://doi.org/10.1016/j.ijepes.2021.107046.
[38] W. Cai, R. Mohammaditab, G. Fathi, K. Wakil, A.G. Ebadi, N. Ghadimi, Optimal bidding and offering strategies of compressed air energy storage: a hybrid robust-stochastic approach, Renew. Energy 143 (2019) 1–8, https://doi.org/10.1016/j.renene.2019.05.008.
[39] X. Zhou, C. Yang, W. Gui, State transition algorithm, J. Ind. Manag. Optim. 8 (2012) 1039–1056, https://doi.org/10.3934/jimo.2012.8.1039.
[40] G. Mokryani, P. Siano, A. Piccolo, Optimal allocation of wind turbines in microgrids by using genetic algorithm, J. Ambient. Intell. Humaniz. Comput. 4 (2013) 613–619, https://doi.org/10.1007/s12652-012-0163-6.
[41] S. Phommixay, M.L. Doumbia, D. Lupien St-Pierre, Review on the cost optimization of microgrids via particle swarm optimization, Int. J. Energy Environ. Eng. 11 (2020) 73–89, https://doi.org/10.1007/s40095-019-00332-1.
[42] A.A. Hafez, A.Y. Abdelaziz, M.A. Hendy, A.F.M. Ali, Optimal sizing of off-line microgrid via hybrid multi-objective simulated annealing particle swarm optimizer, Comput. Electr. Eng. 94 (2021), https://doi.org/10.1016/j.compeleceng.2021.107294.
[43] M. Majidi, B. Mohammadi-Ivatloo, A. Soroudi, Application of information gap decision theory in practical energy problems: a comprehensive review, Appl. Energy 249 (2019) 157–165, https://doi.org/10.1016/j.apenergy.2019.04.144.
[44] S. Nojavan, K. Zare, M.A. Ashpazi, A hybrid approach based on IGDT-MPSO method for optimal bidding strategy of price-taker generation station in day-ahead electricity market, Int. J. Electr. Power Energy Syst. 69 (2015) 335–343, https://doi.org/10.1016/j.ijepes.2015.01.006.
[45] D. Ke, F. Shen, C.Y. Chung, C. Zhang, J. Xu, Y. Sun, Application of information gap decision theory to the design of robust wide-area power system stabilizers considering uncertainties of wind power, IEEE Trans. Sustain. Energy 9 (2018) 805–817, https://doi.org/10.1109/TSTE.2017.2761913.
[46] Y. Ben-Haim, Info-Gap Decision Theory Decisions Under Severe Uncertainty, 2nd ed., Elsevier, 2006 https://doi.org/10.1016/B978-0-12-373552-2.X5000-0.

[47] X. Zhou, C. Yang, W. Gui, A statistical study on parameter selection of operators in continuous state transition algorithm, IEEE Trans. Cybern. 49 (2019) 3722–3730, https://doi.org/10.1109/TCYB.2018.2850350.
[48] A. Soroudi, M. Aien, M. Ehsan, A probabilistic modeling of photo voltaic modules and wind power generation impact on distribution networks, IEEE Syst. J. 6 (2012) 254–259, https://doi.org/10.1109/JSYST.2011.2162994.
[49] N. Aghbalou, A. Charki, S.R. Elazzouzi, K. Reklaoui, A probabilistic assessment approach for wind turbine-site matching, Int. J. Electr. Power Energy Syst. 103 (2018) 497–510, https://doi.org/10.1016/j.ijepes.2018.06.018.
[50] Homer Energy, Homer User Manual, 2016.
[51] J.A. Duffie, W.A. Beckman, Solar Engineering of Thermal Processes, John Wiley & Sons, Inc., Hoboken, NJ, USA, 2013, https://doi.org/10.1002/9781118671603.
[52] C. Monteiro, I.J. Ramirez-Rosado, L.A. Fernandez-Jimenez, M. Ribeiro, New probabilistic price forecasting models: application to the Iberian electricity market, Int. J. Electr. Power Energy Syst. 103 (2018) 483–496, https://doi.org/10.1016/j.ijepes.2018.06.005.
[53] M. Wahbah, B. Mohandes, T.H.M. EL-Fouly, M.S. El Moursi, Unbiased cross-validation kernel density estimation for wind and PV probabilistic modelling, Energy Convers. Manag. 266 (2022) 115811, https://doi.org/10.1016/j.enconman.2022.115811.
[54] A. Tafone, A. Romagnoli, E. Borri, G. Comodi, New parametric performance maps for a novel sizing and selection methodology of a Liquid Air Energy Storage system, Appl. Energy 250 (2019) 1641–1656, https://doi.org/10.1016/j.apenergy.2019.04.171.
[55] R. Morgan, S. Nelmes, E. Gibson, G. Brett, Liquid air energy storage - analysis and first results from a pilot scale demonstration plant, Appl. Energy 137 (2015) 845–853, https://doi.org/10.1016/j.apenergy.2014.07.109.
[56] C. Yan, C. Wang, Y. Hu, M. Yang, H. Xie, Optimal operation strategies of multi-energy systems integrated with liquid air energy storage using information gap decision theory, Int. J. Electr. Power Energy Syst. 132 (2021), https://doi.org/10.1016/j.ijepes.2021.107078.
[57] W.B. Powell, S. Meisel, Tutorial on stochastic optimization in energy - part I: modeling and policies, IEEE Trans. Power Syst. 31 (2016) 1459–1467, https://doi.org/10.1109/TPWRS.2015.2424974.
[58] M.A. Mirzaei, M. Nazari-Heris, B. Mohammadi-Ivatloo, K. Zare, M. Marzband, M. Shafie-Khah, A. Anvari-Moghaddam, J.P.S. Catalao, Network-constrained joint energy and flexible ramping reserve market clearing of power- and heat-based energy systems: a two-stage hybrid igdt-stochastic framework, IEEE Syst. J. 15 (2021) 1547–1556, https://doi.org/10.1109/JSYST.2020.2996952.